Society For Biomaterials

Design and mechanical evaluation of a novel fiber-reinforced scaffold for meniscus replacement

Eric Balint, Charles J. Gatt, Jr., Michael G. Dunn

Orthopaedic Research Laboratories, Department of Orthopaedic Surgery, UMDNJ-Robert Wood Johnson Medical School, New Brunswick, New Jersey 08903

Received 10 January 2011; revised 22 June 2011; accepted 29 August 2011
Published online 23 October 2011 in Wiley Online Library (wileyonlinelibrary.com). DOI: 10.1002/jbm.a.33260

Abstract: A fiber-reinforced degradable scaffold for replacement of meniscal tissue was designed, fabricated, and mechanically evaluated. The hypotheses were that (1) the fiber network design would share a portion of compressive loads via the generation of circumferential tensile loads, and (2) the scaffold tensile properties would be similar to those of the meniscus. Two meniscus scaffold designs varying in fiber content (1000 or 500 fibers: MS1000, MS500) underwent cyclic compressive loading up to 100 and 250*N*, with resultant tensile loads measured at the anterior and posterior anchors. Standard tensile testing was also performed on each device and ovine menisci. Both scaffolds generated tensile loads directly proportional to the applied compressive loads, with MS1000 scaffolds generating approximately twice the tensile loads of MS500 scaffolds. The tensile strength of MS1000 scaffolds was significantly higher than that of the medial and lateral ovine menisci, and approximately twice that of the MS500 scaffolds. The stiffness of MS1000 scaffolds was lower than that of the lateral meniscus, but not statistically different from that of the medial meniscus. These results support our hypotheses that this novel fiber-reinforced scaffold can mimic the tensile and hoop stress behavior of normal meniscal tissue under compressive loading. The circumferential tensile strength and stiffness are appropriate for a meniscus replacement device. © 2011 Wiley Periodicals, Inc. J Biomed Mater Res Part A: 100A: 195–202, 2012.

Key Words: meniscus, scaffold, collagen, polyarylate, biomechanics

How to cite this article: Balint E, Gatt CJ Jr., Dunn MG. 2012. Design and mechanical evaluation of a novel fiber-reinforced scaffold for meniscus replacement. J Biomed Mater Res Part A 2012:100A:195–202.

INTRODUCTION

The meniscus provides protection to the underlying articular cartilage of the knee by transmitting loads through the joint, distributing high peak stresses on the underlying surfaces, providing shock absorption, aiding in joint lubrication, and contributing to overall joint stability.[1–6] Proper function of the tissue is dependent on its geometry, tissue attachments, and a highly organized extracellular matrix (ECM). Located between the femoral condyles and the tibial plateau, the lateral and medial menisci are C-shaped discs of fibrocartilage with a triangular cross-section. The ends of the menisci, or horns, are anchored to the tibial plateau at its anterior and posterior aspects. The tissue is comprised primarily of type I and II collagen fibers arranged in a circumferential pattern. When the meniscus is loaded axially it is compressed and extruded from the joint space. The circumferentially arranged fibers resist this extrusion at the anterior and posterior horn attachments, thus generating forces in the tangential direction. In essence, an axial compressive load is shared as circumferential tensile load within the meniscus.

Investigators have consistently shown the strong correlation between removal of significant amounts of meniscal tissue with degraded joint function as well as the onset of osteoarthritis of the knee.[7–11] To date, no "gold-standard" exists for patients suffering from severe meniscal deficiency. One type of treatment currently being explored by investigators is the use of biocompatible, resorbable scaffolds to replace damaged meniscal tissue.[12–17] Several types of scaffolds made up of collagen and various polymers in sponge form are currently being developed. While some of these devices have shown promising preliminary data, none have been widely accepted by the orthopaedic community. The isotropic properties inherent to sponges prevent these

Correspondence to: M. G. Dunn; e-mail: dunnmg@umdnj.edu
Contract grant sponsor: National Institutes of Health (NIH); contract grant number: R21 AR052118
Contract grant sponsor: NJ Center for Biomaterials—Center for Military Biomaterials Research (CeMBR); contract grant number: W81XWH042003
Contract grant sponsor: Armed Forces Institute of Regenerative Medicine (AFIRM, Rutgers-Cleveland Clinic Consortium); contract grant number: W81XWH-08-2-0034
Contract grant sponsors: National Institute of Arthritis and Musculoskeletal and Skin Diseases (NIAMS), UMDNJ NJCST Technology Commercialization Fund, Summer Research Fellowships

scaffolds from mimicking the load-bearing role of highly anisotropic tissues such as the meniscus, and limit their use in instances where full meniscectomies are required.[18]

Our lab is developing a resorbable scaffold to replace severely damaged meniscal tissue. This novel design is based on the microstructure of the normal meniscus, with an emphasis on providing circumferential tensile strength. The scaffold is comprised of a type I collagen sponge reinforced with resorbable synthetic polymer fibers. Collagen is a useful biomaterial for musculoskeletal tissue engineering due to its unique biochemical and mechanical properties.[19] Its high cellular affinity makes it an ideal coating material for synthetic polymers, which lack cell-recognition signals. Furthermore, the mechanical strength, degradation profile, and porosity of collagen implants can be controlled by various methods of crosslinking. The fiber component of this scaffold is made of a biodegradable, tyrosine derived synthetic polymer.[20,21] Compared to other polymers considered, it has a relatively high ultimate stress and low modulus of elasticity, making it an ideal candidate for applications where high stresses and strains are likely to be encountered.

In this study, two potential designs differing in the amount of reinforcing fiber were evaluated mechanically. Two hypotheses related to the mechanical function of scaffolds were tested: (1) Fiber-reinforced meniscus scaffolds would share a portion of an axial compressive load via the generation of circumferential tensile load and (2) Fiber-reinforced meniscus scaffolds would possess circumferential tensile properties similar to those of the normal ovine meniscus. A scaffold that can temporarily replace the load-bearing function of the meniscus while inducing formation of neo-meniscal tissue would offer a promising alternative to patients suffering from severe meniscal deficiency.

METHODS

Scaffold fabrication

The size, shape, and geometry of scaffolds were based on those of an adult ovine meniscus, the animal model to be used in subsequent meniscal replacement surgeries. The raw materials for the scaffolds were acid-insoluble bovine dermal collagen (Nitta Casings, Somerville, NJ) reinforced by a network of degradable tyrosine-derived polymer fibers, poly(desaminotyrosyl-tyrosine dodecyl ester dodecanoate),[12,10] or p(DTD DD). The polymer fiber was melt-extruded by the New Jersey Center for Biomaterials, (Rutgers University, Department of Chemistry) as previously described.[22] The resultant fiber had an average diameter of 80 μm, yield stress of 150 MPa, and a modulus of 1.7 GPa. For each scaffold, a continuous length of this fiber was wrapped in a quasi-circumferential three-dimensional pattern indicated in Figure 1. Two types of scaffolds were fabricated differing in the number of passes of the pattern, or cross-sectional fiber count: 500 fiber scaffolds (MS500) and 1000 fiber scaffolds (MS1000). MS500 scaffolds contained ~120 mg or 45 m of polymer fiber, while MS1000 scaffolds contained ~240 mg or 90 m, the maximum amount that would fit into a device constrained by these dimensions.

A peripheral mold was formed around the outer edge of the fiber assembly and a 1% (w/v) collagen dispersion injected into it. The assembly was frozen in an ethanol-dry ice bath and then lyophilized. To increase the structural integrity of the implant and minimize fiber slippage, a continuous length of polymer fiber (~200 cm) was threaded repeatedly through the periphery. Scaffolds were crosslinked in a 1-ethyl-3-(dimethyl aminopropyl) carbodiimide (EDC) solution per a protocol used previously in our lab.[23,24] Scaffolds were extensively rinsed and again lyophilized, then transferred to sealable pouches and sterilized with electron-beam irradiation (25 kGy). Sterile scaffolds were stored in a dark vacuum chamber until use. Figure 1 shows a complete MS1000 scaffold prior to mechanical testing.

Mechanical characterization of meniscal scaffolds

The meniscus is a complex tissue, with mechanical requirements and properties combining those of ligaments and cartilage. The purpose of the following experiments was to characterize the structural properties of fiber-reinforced scaffolds and determine their potential utility as a biomechanically relevant meniscal implant.

Load sharing of axial compressive loads by generation of circumferential tensile loads

To determine the ability of scaffolds to share compressive loads via the generation of tensile loads, two Instron mechanical testing systems (Norwood, MA) were used: (1) Model #5569, 10-k*N* load cell, Bluehill software, for the application of a compressive load and (2) Model #5542, 100*N* load cell, Merlin software, for the measurement of the resultant tensile load. Figure 2 shows the setup of the dual Instron system prior to testing. A customized jig was fabricated for use with the Instron 5569. The distal and proximal four inches of an ovine femur and tibia, respectively, were harvested, stripped of all soft tissues, dehydrated, and then coated with a thin layer of polyurethane glue. A threaded steel rod was inserted into the midline of each to secure to aluminum frames which coupled with the Instron 5569, 10 k*N* load cell. Two bone tunnels were drilled through the tibia, originating at the anterior and posterior horn attachments on the tibial plateau, and exiting out the lateral aspect of the tibial shaft. These were used for insertion and fixation of the meniscus scaffolds to the tibial plateau. For each test run, the femoral and tibial jigs were loaded into the Instron 5569 at a 30° angle. One MS500 and one MS1000 scaffold were initially fabricated and then utilized to determine the optimal positioning, fixation, and pretensioning for this experimental protocol. Once a useful procedure was well established, these scaffolds were discarded.

Ethibond suture (size 5; Ethicon, Somerville, NJ) was chosen for the anchors of this scaffold due to its relatively high strength and modulus as compared to the polymer fibers. Two loops of suture were threaded through the anterior and posterior horns of a meniscus scaffold and then fed into the bone tunnels, along with ~1 cm of each scaffold

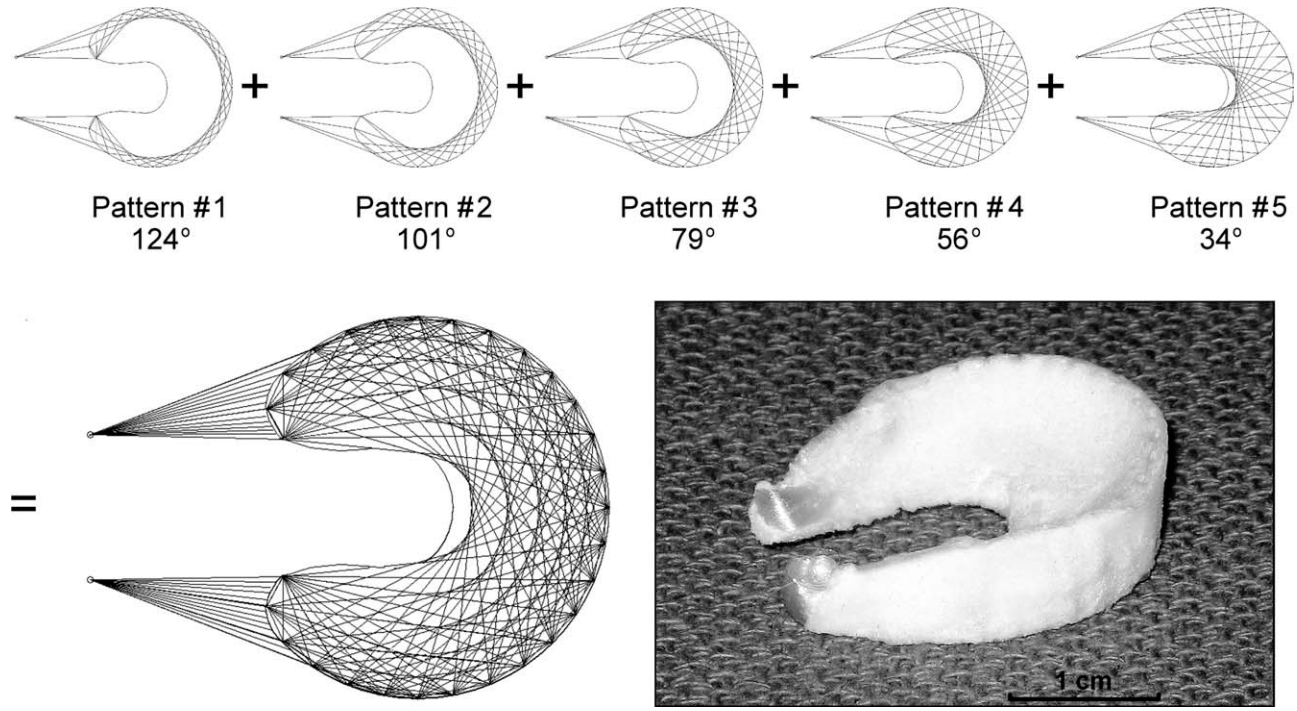

FIGURE 1. Fiber weaving pattern used for scaffolds with picture of complete MS1000 scaffold. The given measurement for each pattern is the angle at which the fiber bends around each node. For each scaffold, these patterns were arranged in a manner to obtain the wedge-shaped cross-section of the meniscus, with lower angle patterns predominant near the base and higher angles at the apex.

horn. The suture was secured to a light-weight, high strength steel cable (Φ: 1/32", 3 × 7 hollow-core, McMaster-Carr, Robbinsville, NJ) on the opposite side of the tunnel. This cable was fed through a high precision pulley (McMaster-Carr, Robbinsville, NJ) attached to the bottom plate of the Instron 5542, and secured to its 100*N* load cell. Once loaded into the mechanical testing system, scaffolds were pretensioned to 2*N* by jogging the Instron 5542 crosshead up or down to remove any slack in the suture.

Two experimental groups were evaluated in this experiment: (1) MS500 meniscus scaffolds ($n = 4$) and (2) MS1000 ($n = 4$) meniscus scaffolds. All scaffolds were hydrated in phosphate buffered saline (PBS) for at least 20 min immediately prior to testing. The Instron #5569 applied two loading cycles to each scaffold. The first run was for five cycles with minimum and maximum loads of 10 and 100*N*, respectively. The second run was for five cycles ranging between 10 and 250*N*. Between runs, scaffolds were rehydrated, repositioned, and retensioned. This process typically took between 60 and 90 s. The Instron #5569 collected time and compressive load data while the Instron #5542 collected time and tensile load data. As a blank control, this procedure was also performed with the steel rope secured to the tibia jig through the anterior and posterior bone tunnels.

Circumferential tensile testing

The purpose of this experiment was to quantify the circumferential tensile properties of each type of meniscus scaffold for comparison to the normal ovine meniscus. All testing was performed using an Instron Model #5569 with a 10 k*N* load cell. The following groups were evaluated in this experiment: (1) MS500 meniscus scaffolds ($n = 4$), (2) MS1000 meniscus scaffolds ($n = 4$), (3) medial menisci from knees of skeletally mature sheep ($n = 9$), and (4) lateral menisci from knees of skeletally mature sheep ($n = 9$).

All test samples were hydrated in PBS at room temperature. To mitigate failure by crack propagation in the native meniscus samples, 1–2 mm of the translucent tissue at the inner margin was trimmed away. Approximately 5 mm of each sample was loaded into cryogenic freeze clamps (Enduratec, Eden Prairie, MN). While freezing, samples were pretensioned to 2*N*, resulting in a gauge length between 8 and 12 mm. While the testable area remained unfrozen, samples were pulled until failure at a constant rate of 10 mm min^{-1}. For each test run, the time, deformation, and tensile load were recorded.

Statistical analysis

Data were analyzed statistically with a one-way ANOVA and multiple pairwise comparisons determined using the Student–Newman–Keuls Method. p values <0.05 were considered statistically significant. Calculations were performed using Sigma-Stat software.

RESULTS

Load sharing of axial compressive loads by generation of circumferential tensile loads

A direct correlation was observed between the compressive load applied to scaffolds and the resultant tensile load

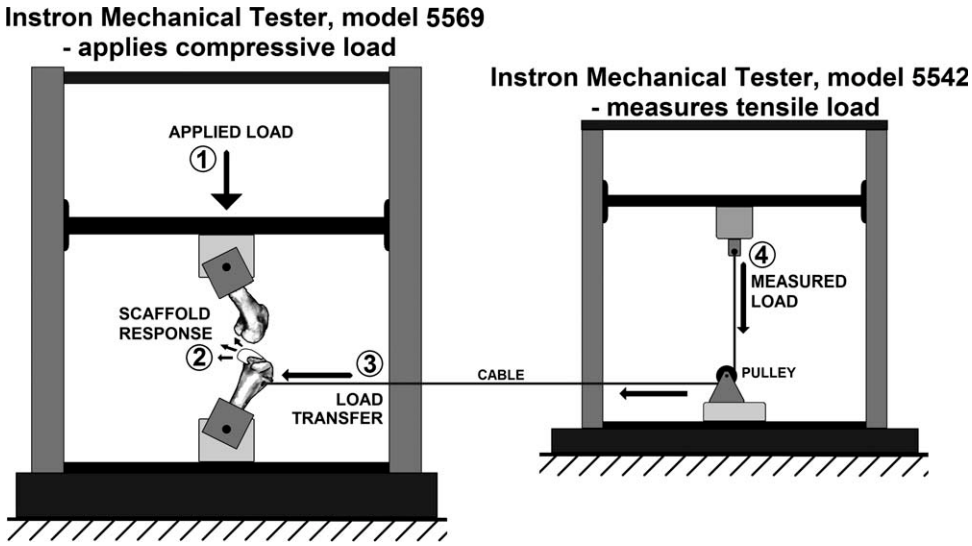

FIGURE 2. Mechanical testing system setup. (1) The Instron Model #5569 (left) applied a compressive load at a constant rate up to 250*N*. (2) In response to the applied compressive load, the scaffold generated tensile loads. (3) The tensile loads were transferred through the braided steel cable and (4) measured at the load cell of the Instron Model #5542 (right). Compressive and tensile loads were recorded by the load cells every 0.1 s.

measured at the anterior and posterior anchor attachments. Figure 3 shows typical results for each of the scaffold designs under 10–100*N* and 10–250*N* cyclic loading as well as loading in the presence of no scaffold (blank control). On the first cycle, measured tensile values increased from the pretension value of $\sim 2N$ to a certain maximum value. Subsequent increases and decreases in the applied compressive load were reflected by similar changes in the measured tensile loads. The measured minimum and maximum tensile loads within the body of the cyclic run always remained above the initial pretension value. On the final cycle of the 100 and 250*N* runs, the compressive load was increased to 150 and 260*N*, respectively, and then completely removed from the tibial jig. After removal, the measured tensile load on the anterior and posterior anchor attachments returned to approximately the pretension value. Cyclic loading in the presence of no scaffold revealed a relatively minor contribution to the measured tensile load from deformation of the tibial jig.

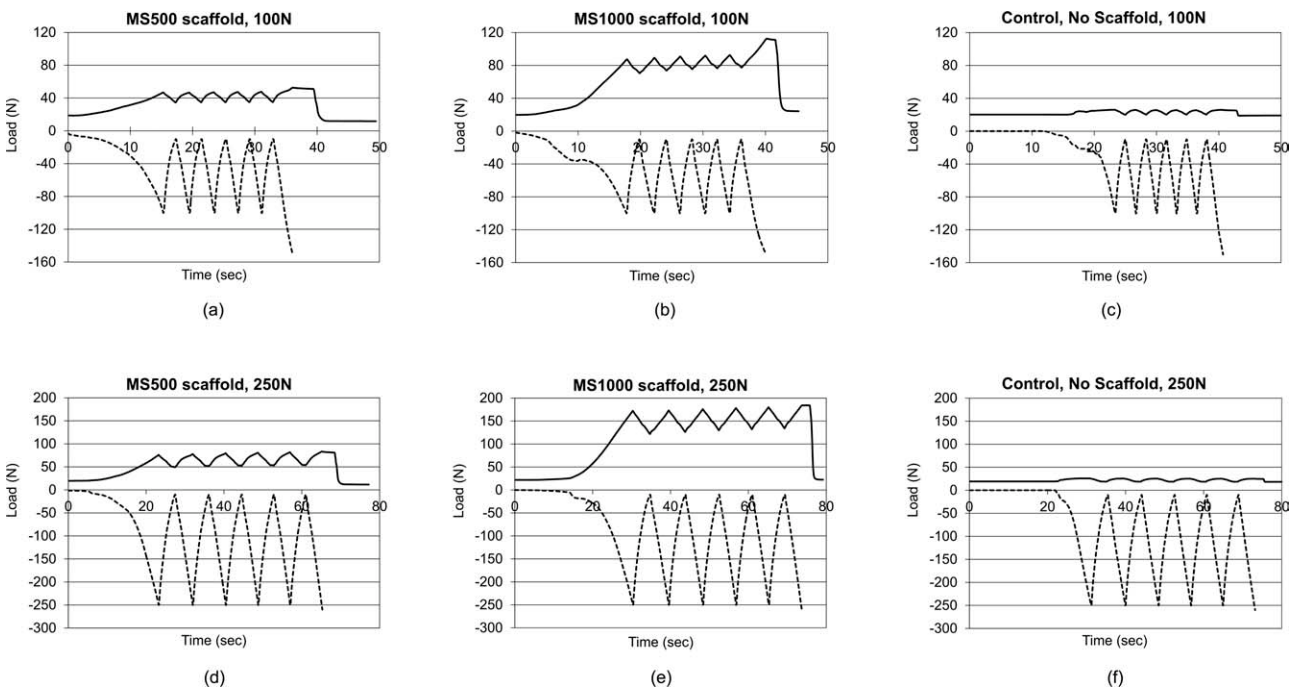

FIGURE 3. Applied compressive load (bottom dotted line) as compared to 10× the measured tensile load (top solid line) for one of each scaffold type under each cyclic loading condition. Results are typical for each scaffold evaluated. For each scaffold, there was a direct correlation between the applied compressive load and the measured tensile load.

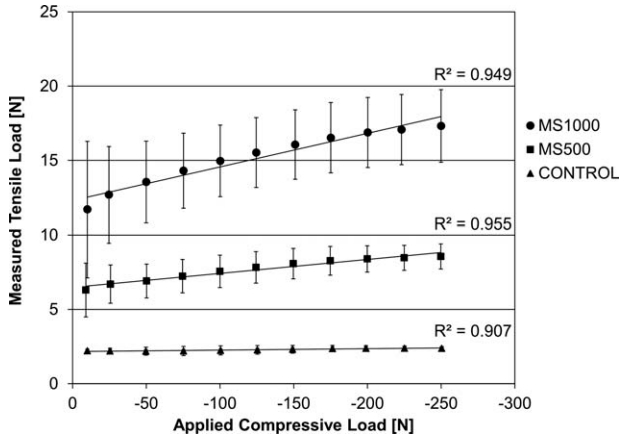

FIGURE 4. Relationship between the applied compressive load and the measured tensile load for the 250*N* runs. Linear trendlines for each cyclic load run are included, with corresponding R^2 values. Error bars represent standard deviations. For compressive loads above 10*N*, significant differences ($p < 0.05$) were observed between the tensile loads generated in the different scaffold groups.

For MS500 scaffolds, the average maximum tensile load measured during the 100*N* cycle was 6.0 ± 1.0 *N*, and 9.1 ± 0.6 *N* for the 250*N* cycle. Likewise, the average maximum tensile loads for MS1000 scaffolds were 10.2 ± 1.2*N* and 17.8 ± 2.4*N*, respectively. The maximum tensile loads generated in the scaffolds were significantly ($p < 0.05$) influenced by scaffold type and cyclic loading level. For MS500 scaffolds, the average difference in measured tensile load at the minimum and maximum compressive loads for the 100 and 250*N* cycles was 1.2 ± 0.1*N* and 2.9 ± 0.3*N*, respectively. Similarly for MS1000 scaffolds, the average difference was 2.1 ± 0.7 *N* and 5.3 ± 1.8 *N*. Again, these differences were statistically significant ($p < 0.05$).

For the 250*N* cyclic load runs, the average measured tensile load at regular intervals was plotted against the corresponding applied compressive load (Fig. 4). For MS500 and MS1000 scaffolds, 24 data points were averaged for the 10 and 250*N* compressive loads. For all other compressive loads, 44 data points were averaged. For the control group, six data points were averaged for 10 and 250*N*, while 11 were averaged for all other loads. A linear relationship was calculated between generated tensile load versus applied compressive load, and the corresponding trendline and R^2 value are shown in Figure 4 for each scaffold type (MS500, MS1000, blank control). At applied compressive loads above 10*N*, the tensile loads generated in each group were significantly different ($p < 0.05$).

Circumferential tensile testing

In this experiment, the structural properties of scaffolds were evaluated and compared to those of the normal ovine meniscus. Figure 5 shows the tensile load at yield and the stiffness of scaffolds and ovine menisci. The yield load of MS500 and MS1000 scaffolds was 348 and 828*N*, respectively, while that of the medial and lateral ovine meniscus was 552 and 579*N*, respectively. MS1000 scaffolds had a significantly higher yield load ($p < 0.05$) than MS500 scaffolds and both lateral and medial ovine menisci.

The stiffness of MS500 and MS1000 scaffolds was 108 and 136 $N\ mm^{-1}$. That of the medial and lateral menisci was 147 and 232 $N\ mm^{-1}$, respectively. Lateral menisci had a significantly higher stiffness ($p < 0.05$) than that of all other groups. The stiffness of the medial meniscus was also found to be higher than that of the MS500 scaffolds ($p < 0.05$). No other significant differences were found.

DISCUSSION

From a biomechanical standpoint, the meniscus can be considered one of the most complex soft tissues in the body. It undergoes a myriad of stresses and strains which dictate its microstructure and function, as well as the overall health of the surrounding structures.[25–30] In this study, a novel fiber-reinforced meniscal analog was evaluated biomechanically to determine its potential utility as a load-bearing device in the knee, with a focus on determining its tensile response to axial, compressive loads.

Several investigators have experimented with various materials in sponge form for meniscal replacement—concentrating primarily on compressive loading.[15,16,31–33] While resorbable polymer mesh scaffolds have been used by several investigators as meniscus replacements, data on these devices is limited to *in vitro* cytocompatibility[34,35] and testing in small animal models.[13] While Chari et al. and Kon et al. did consider circumferential reinforcement in the development of their meniscal scaffolds,[12,14] the fiber reinforcement was limited and used primarily for attachment of the scaffold to the stumps of the resected meniscus.

In this study, the assessment of the meniscus scaffold function focused on the tensile loads generated in the scaffold in response to axial loads across the knee joint. The hoop-stress theory of meniscus function states that axial

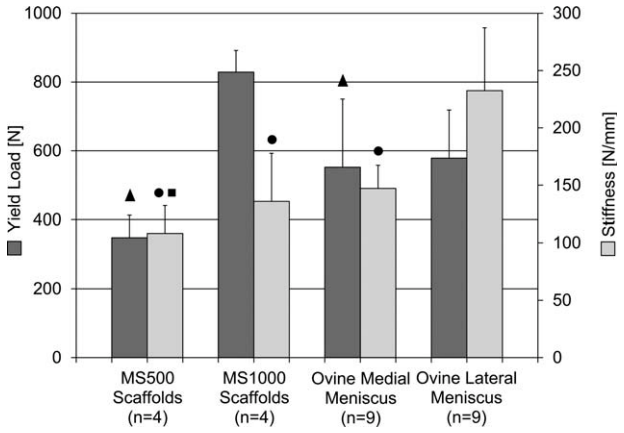

FIGURE 5. Structural tensile properties of scaffolds and native ovine meniscal tissue tested in tension to failure. Error bars represent standard deviations. A one-way ANOVA was performed on this data set and pairwise comparisons made with the Student–Newman–Keuls method. Significant differences ($p < 0.05$) with relation to the MS1000 scaffolds are noted by a triangle; with relation to the Lateral Menisci are noted by a circle; and with relation to the Medial Menisci are noted by a square.

compressive loads are resisted by the generation of circumferentially oriented tensile stresses originating at the anterior and posterior horns of the tissue.[36] Therefore, a resorbable scaffold with robust circumferential fiber-reinforcement was designed and evaluated mechanically to determine the extent to which it could mimic the mechanical function of the normal meniscus. Because the structural behavior of the meniscus is highly dependent on its geometry, the overall shape and dimensions of the meniscus scaffold were modeled after those of the normal tissue. A wedge-shaped cross-section was obtained by creating a nonuniform fiber distribution pattern, in which specific low-angle weaves were employed near the base of the device, and high-angle weaves were used at its apex. The ends of the scaffolds were extended to form high strength, fibrous tissue anchors which were continuous with the fiber reinforcement within the main body of the device. These anchor attachments, coupled with the proper scaffold geometry, were critical for the creation of a device with the potential to share axial loads across the knee joint by the generation of tensile forces in the meniscus scaffold.

Early prototypes of the scaffold varied in fiber distribution pattern and content. One potential pattern included a layered mesh design which was easily fabricated with reproducible properties, but lacked a method for incorporating strong anchor attachments. Another was a purely circumferential pattern. However, difficulties in securing bundles of fibers together into a cohesive device caused this design to be discarded. The quasi-circumferential pattern utilized in this study incorporated strong anchor attachments into its design with reproducible mechanical properties, yet was labor intensive to construct. Future studies will utilize textile methods to optimize fabrication of this design and alternative circumferential fiber orientation patterns.

In the first experiment, a five cycle loading regimen was employed to simulate repetitive loading in the hind-limb of a quadruped. The 100*N* cycle represented a relatively low stress condition (such as simple weight-bearing), while the 250*N* cycle represented a higher stress condition (such as walking or jogging). Both scaffold designs were able to withstand the repetitive loading without significant, permanent deformation. They maintained their semi-lunar shape and wedge cross-section throughout the evaluation. Furthermore, the collagen matrix around the fibers did not degenerate or wear away appreciably after repetitive loading.

Results from this experiment support the first hypothesis by showing that fiber-reinforced meniscus scaffolds loaded axially in compression responded with the generation of circumferentially oriented tensile loads measured directly at the anterior and posterior scaffold horn attachments. The percentage of generated tensile load approximately doubled between MS500 and MS1000 scaffolds—likely due to the increased fiber density of MS1000 scaffolds. This increase may indicate that a greater percentage of the MS1000 scaffold is undergoing tensile stress in response to the compressive loading. Theoretically, during remodeling of neo-tissue replacing the scaffold *in vivo*, these tensile stresses may induce the growth of a more fibrocartilagenous tissue similar to that found in the normal meniscus. Furthermore, the increase in tensile stresses suggests that MS1000 scaffolds may decrease compressive loads on the tibial plateau, protecting the cartilage from damage. Further *in vivo* testing in a large animal model would be required to determine the characteristics of the neo-tissue formed as well as its effects on the articular surfaces.

To our knowledge, no other group has directly measured the tensile loads generated in a meniscus (or meniscus analog) as a result of axial compressive loading. Studies have instead focused primarily on the measurement of hoop strains of menisci through the use of a strain gauge.[37–39] For this type of scaffold where a spongy matrix was involved, a strain gauge was found to be impractical since its barbs could not adhere to the load-bearing portion of the scaffold—the polymer fibers.

In the second experiment, scaffolds and ovine menisci were pulled to failure to compare their structural properties. The results supported the second hypothesis, as the properties of both scaffold designs fell within range of the ovine menisci with regards to overall yield load and stiffness. MS1000 scaffolds had significantly greater yield loads than either the MS500 scaffolds or the ovine menisci, but had comparable stiffness. Based on previous data generated in our lab which looked at the performance of resorbable scaffolds in a synovial environment,[23,40–42] it is anticipated that there will be a significant reduction in mechanical properties after implantation of meniscal scaffolds in the synovial environment. From a biomechanical perspective, this may allow the MS1000 scaffold design to function mechanically in the joint for a longer period of time than an implant with a lower yield load.

The polymer used to create the fiber network is also currently being explored by our lab in the development of a scaffold for anterior cruciate ligament reconstruction.[22] The relatively high strength and low modulus of p(DTD DD) makes it an ideal candidate in applications where repetitive loading occurs. The polymer fiber network utilized in this study resulted in scaffolds with initial structural properties appropriate for meniscus replacement. However, utilizing alternative degradable polymers with similar mechanical properties and resorption profile to fabricate meniscus scaffolds may produce comparable results.

There were several limitations to the experiments conducted in this study. In the load sharing experiment, no additional soft tissue stabilization was present (i.e., cruciate and collateral ligaments, lateral meniscus or meniscocapsular attachments). Radin et al. demonstrated that any abnormality in the knee joint—such as missing tissues—would result in irregular loading conditions.[43] The key implication in this first experiment is that fiber reinforced scaffolds do have the ability to share axial compressive loads via the generation of circumferential tensile loads. This data is valid only for preimplanted scaffolds and gives no indication on whether or not this behavior would persist after short- or long-term implantation in a synovial environment.

Because of the nature of the scaffolds, it was impractical to harvest small, dog-bone-shaped samples for material property testing in the second experiment. Instead, the structural properties were evaluated by pulling the entire scaffold or meniscus in tension. This protocol is similar to that used by Newman et al., who tested whole menisci in tension after trimming away the inner margin and outer periphery.[44] While the low length-to-width ratio of test samples inherent to this procedure is a potential source of error, these results do suggest that both scaffold designs have initial structural tensile properties similar to those of the normal ovine meniscus. Another consequence of this scaffold design was the impracticality of conducting standard compression testing. Because of the high porosity of the collagen sponge around the fiber network, as well as its relatively low strength compared to polymer fiber, cylindrical samples could not be stabilized for testing.

The number of samples evaluated in both experiments was limited by the amount of polymer fiber available for use. Based on this, as well as the amount of fiber per scaffold, it was determined that five of each type of scaffold could be fabricated. Because of the novelty of the load transfer evaluation, one scaffold from each group was sacrificed to determine the optimal parameters for this analysis, leaving four scaffolds per group for analysis and data collection. Based on preliminary results from the sacrificed samples, as well as previous single-fiber data (not published), an analysis was performed to determine the power of an experiment with an alpha level of 0.05 and a sample size of 4. For the load sharing experiment, it was assumed that the average tensile load generated in response to the applied compressive load for MS500 scaffolds was $\sim$60% of that of MS1000 scaffolds. Assuming a common standard deviation of 20% and a sample size of 4, the calculated power was 0.81. For the tensile strength analysis, single fiber data was used to estimate an average tensile strength of 400*N* for MS500 scaffolds, and 800*N* for MS1000 scaffolds. A conservative standard deviation of 150*N* was considered with a sample size of 4, resulting in a power of 0.96. Because of the relatively large difference in fiber count between MS500 and MS1000 scaffolds, the statistically significant differences in their mechanical behavior were not unexpected.

MS1000 scaffolds represented the highest fiber density attainable for a scaffold reinforced with the described quasi-circumferential fiber pattern and constrained by the dimensions of an ovine meniscus. One potential concern with this design is that high fiber density might impede cellular and tissue ingrowth within the scaffold, thus delaying its incorporation and promoting an encapsulation response. While MS500 scaffolds possess significantly lower tensile properties than MS1000 scaffolds, they have a lower fiber density, which may allow for increased cell proliferation into the implant, potentially improving the overall biological response to the device. This possible trade-off between mechanical strength and biological incorporation will be explored further in *in vitro* and *in vivo* biocompatibility and efficacy studies.

CONCLUSION

This article describes the design, fabrication, and mechanical evaluation of a novel polymer fiber-reinforced collagen scaffold for use as a meniscal replacement. The long-term goal of this research is to develop a resorbable scaffold which can be used after a subtotal or total meniscectomy to induce neofibrocartilaginous tissue growth while preventing or delaying the onset of degenerative changes of the articular surfaces.

Fiber-reinforced meniscus scaffolds were found to (1) share axial compressive loads via generation of circumferential tensile loads within the scaffold and (2) possess circumferential tensile properties within the range of the normal ovine meniscus. From a biomechanical standpoint, this device has the potential to assume a load-bearing role in the knee if used as a temporary, remodelable scaffold to replace surgically removed meniscal tissue.

REFERENCES

1. Ahmed A. The load-bearing role of knee menisci. In: Mow V, Arnoczky S, Jackson D, editors. Knee Meniscus: Basic and Clinical Foundations. New York, NY: Raven; 1992. p 59–73.
2. King D. The function of semilunar cartilages. J Bone Joint Surg 1936;18:1069–1076.
3. Renstrom P, Johnson RJ. Anatomy and biomechanics of the menisci. Clin Sports Med 1990;9:523–538.
4. Seedhom B, Hargreaves D. Transmission of the load in the knee joint with special reference to the role of menisci. Eng med 1979; 8:220–228.
5. Shrive NG, O'Connor JJ, Goodfellow JW. Load-bearing in the knee joint. Clin Orthop Relat Res 1978;131:279–287.
6. Walker P, Erkman M. Role of the menisci in force transmission across the knee. Clin Orthop 1975;109:184–192.
7. Casscells SW. The torn or degenerated meniscus and its relationship to degeneration of the weight-bearing areas of the femur and tibia. Clin Orthop Relat Res 1978;132:196–200.
8. Fairbank T. Knee joint changes after meniscectomy. J Bone Joint Surg (Br) 1948;30:664–670.
9. Krause W, Pope M, Johnson R, Wilder D. Mechanical changes in the knee after meniscectomy. J Bone Joint Surg 1976;58:599–604.
10. Bylski-Austrow D, Malumed J, Meade T, Grood E. Knee joint contact pressure decreases after chronic meniscectomy relative to acutely meniscectomized joints: A mechanical study in the goat. J Ortho Res 1993;11:796–804.
11. Cox JS, Nye CE, Schaefer WW, Woodstein IJ. The degenerative effects of partial and total resection of the medial meniscus in dogs' knees. Clin Orthop 1975;109:178–183.
12. Chiari C, Koller U, Dorotka R, Eder C, Plasenzotti R, Lang S, Ambrosio L, Tognana E, Kon E, Salter D, Nehrer S. A tissue engineering approach to meniscus regeneration in a sheep model. Osteoarthritis Cartilage 2006;14:1056–1065.
13. Kang SW, Son SM, Lee JS, Lee ES, Lee KY, Park SG, Park JH, Kim BS. Regeneration of whole meniscus using meniscal cells and polymer scaffolds in a rabbit total meniscectomy model. J Biomed Mater Res A 2006;78:659–671.
14. Kon E, Chiari C, Marcacci M, Delcogliano M, Salter DM, Martin I, Ambrosio L, Fini M, Tschon M, Tognana E, Plasenzotti R, Nehrer S. Tissue engineering for total meniscal substitution: Animal study in sheep model. Tissue Eng Part A 2008;14:1067–1080.
15. Stone KR, Steadman JR, Rodkey WG, Li ST. Regeneration of meniscal cartilage with use of a collagen scaffold. Analysis of preliminary data. J Bone Joint Surg Am 1997;79:1770–1777.
16. Tienen TG, Heijkants RG, Buma P, De Groot JH, Pennings AJ, Veth RP. A porous polymer scaffold for meniscal lesion repair—A study in dogs. Biomaterials 2003;24:2541–8.
17. Welsing RT, van Tienen TG, Ramrattan N, Heijkants R, Schouten AJ, Veth RP, Buma P. Effect on tissue differentiation and articular

cartilage degradation of a polymer meniscus implant: A 2-year follow-up study in dogs. Am J Sports Med 2008;36:1978–1989.
18. Buma P, van Tienen T, Veth R. The collagen meniscus implant. Expert Rev Med Devices 2007;4:507–516.
19. Stenzel KH, Miyata T, Rubin AL. Collagen as a biomaterial. Annu Rev Biophys Bioeng 1974;3:231–253.
20. Bourke SL, Kohn J. Polymers derived from the amino acid L-tyrosine: Polycarbonates, polyarylates and copolymers with poly(ethylene glycol). Adv Drug Deliv Rev 2003;55:447–466.
21. Brocchini S, James K, Tangpasuthadol V, Kohn J. Structure-property correlations in a combinatorial library of degradable biomaterials. J Biomed Mater Res 1998;42:66–75.
22. Tovar N, Bourke S, Jaffe M, Murthy NS, Kohn J, Gatt C, Dunn MG. A comparison of degradable synthetic polymer fibers for anterior cruciate ligament reconstruction. J Biomed Mater Res A 2010;93:738–747.
23. Caruso AB, Dunn MG. Functional evaluation of collagen fiber scaffolds for ACL reconstruction: Cyclic loading in proteolytic enzyme solutions. J Biomed Mater Res 2004;69A:164–171.
24. Caruso AB. A collagen fiber tissue engineering scaffold for anterior cruciate ligament reconstruction [doctorate]. New Brunswick: Rutgers University/University of Medicine and Dentistry of New Jersey; 2004. 148 p.
25. Fermor B, Jeffcoat D, Hennerbichler A, Pisetsky DS, Weinberg JB, Guilak F. The effects of cyclic mechanical strain and tumor necrosis factor alpha on the response of cells of the meniscus. Osteoarthritis Cartilage 2004;12:956–962.
26. Fink C, Fermor B, Weinberg JB, Pisetsky DS, Misukonis MA, Guilak F. The effect of dynamic mechanical compression on nitric oxide production in the meniscus. Osteoarthritis Cartilage 2001;9:481–487.
27. Imler SM, Doshi AN, Levenston ME. Combined effects of growth factors and static mechanical compression on meniscus explant biosynthesis. Osteoarthritis Cartilage 2004;12:736–744.
28. Setton LA, Guilak F, Hsu EW, Vail TP. Biomechanical factors in tissue engineered meniscal repair. Clin Orthop 1999 (367 Suppl): S254–S272.
29. Shin SJ, Fermor B, Weinberg JB, Pisetsky DS, Guilak F. Regulation of matrix turnover in meniscal explants: Role of mechanical stress, interleukin-1, and nitric oxide. J Appl Physiol 2003;95:308–313.
30. Upton ML, Chen J, Guilak F, Setton LA. Differential effects of static and dynamic compression on meniscal cell gene expression. J Orthop Res 2003;21:963–969.
31. Rodkey WG, Steadman JR, Li ST. A clinical study of collagen meniscus implants to restore the injured meniscus. Clin Orthop Relat Res 1999;367:S281–S292.
32. Stone KR, Rodkey WG, Webber R, McKinney L, Steadman JR. Meniscal regeneration with copolymeric collagen scaffolds. In vitro and in vivo studies evaluated clinically, histologically, and biochemically. Am J Sports Med 1992;20:104–111.
33. Tienen TG, Heijkants RG, de Groot JH, Schouten AJ, Pennings AJ, Veth RP, Buma P. Meniscal replacement in dogs. Tissue regeneration in two different materials with similar properties. J Biomed Mater Res B Appl Biomater 2005;76:389–396.
34. Aufderheide AC, Athanasiou KA. Comparison of scaffolds and culture conditions for tissue engineering of the knee meniscus. Tissue Eng 2005;11:1095–1104.
35. Baker BM, Mauck RL. The effect of nanofiber alignment on the maturation of engineered meniscus constructs. Biomaterials 2007; 28:1967–1977.
36. Mow V, Ratcliffe A, Chern K, Kelly M. Structure and function relationships of the menisci of the knee. In: Mow V,Arnoczky S, Jackson D, editors. Knee Meniscus: Basic and Clinical Foundations. New York: Raven Press; 1992. p 37–57.
37. Ahmed AM, Burke DL. In-vitro measurement of static pressure distribution in synovial joints—Part I: Tibial surface of the knee. J Biomech Eng 1983;105:216–225.
38. Jones RS, Keene GC, Learmonth DJ, Bickerstaff D, Nawana NS, Costi JJ, Pearcy MJ. Direct measurement of hoop strains in the intact and torn human medial meniscus. Clin Biomech (Bristol, Avon) 1996;11:295–300.
39. Richards C. A novel approach to measurement of human meniscal strain. New Brunswick: Rutgers University, Graduate School of New Brunswick; 2002. 100 p.
40. Caruso AB, Dunn MG. Changes in mechanical properties and cellularity during long-term culture of collagen fiber ACL reconstruction scaffolds. J Biomed Mater Res A 2005;73:388–397.
41. Dunn MG, Liesch JB, Tiku ML, Zawadsky JP. Development of fibroblast-seeded ligament analogs for ACL reconstruction. J Biomed Mater Res 1995;29:1363–1371.
42. Dunn MG, Tria AJ, Kato YP, Bechler JR, Ochner RS, Zawadsky JP, Silver FH. Anterior cruciate ligament reconstruction using a composite collagenous prosthesis. A biomechanical and histologic study in rabbits. Am J Sports Med 1992;20: 507–515.
43. Radin EL, Bryan RS. The effect of weight-bearing on regrowth of the medial meniscus after meniscectomy. J Trauma 1970;10: 169–175.
44. Newman AP, Anderson DR, Daniels AU, Dales MC. Mechanics of the healed meniscus in a canine model. Am J Sports Med 1989; 17:164–175.